Deciphering the genetic basis of wheat seminal root anatomy uncovers ancestral axial conductance alleles

Elisha Hendel[1,2,#], Harel Bacher[1,3,#], Adi Oksenberg[1], Harkamal Walia[3], Nimrod Schwartz[2], and Zvi Peleg[1,*]

[1.] The Robert H. Smith Institute of Plant Sciences and Genetics in Agriculture, The Hebrew University of Jerusalem, Rehovot 7610001, Israel.

[2.] The Institute of Environmental Sciences, The Hebrew University of Jerusalem, Rehovot 7610001, Israel.

[3.] Department of Agronomy and Horticulture, University of Nebraska-Lincoln, Lincoln, 68583 NE, USA.

[#] These authors equally contributed to this work.

Correspondence: Zvi Peleg,

The Robert H. Smith Institute of Plant Sciences and Genetics in Agriculture,

The Hebrew University of Jerusalem. P.O. Box 12, Rehovot 7610001, Israel.

Tel: +972-8-9489638;

Email: zvi.peleg@mail.huji.ac.il

ABSTRACT

Root axial conductance contributes to the rate of water uptake from the soil throughout the whole plant lifecycle. In a rainfed wheat agro-system, grain-filling is typically occurs during declining water availability (i.e. terminal drought). Therefore, preserving soil water moisture during grain filling could serve as a key adaptive trait. We hypothesized that lower wheat root axial conductance can promote higher yields under terminal drought. A segregating population derived from a cross between durum wheat and its direct progenitor wild emmer wheat was used to underpinning the genetic basis of seminal root architectural and functional traits. We detected 75 QTL associated with seminal roots morphological, anatomical and physiological traits, with several hotspots harboring co-localized QTL. We further validated the axial conductance and central metaxylem QTL using wild introgression lines. Field-based characterization of genotypes with contrasting axial conductance, suggested the contribution of low axial conductance as a mechanism for water conservation during grain filling and consequent increase in grain size and yield. Our findings underscore the potential of introducing wild alleles to reshape the wheat root system architecture for greater adaptability under changing climate.

Key words: Axial conductance, QTL, root anatomy, root hair, wild emmer wheat, wheat seminal roots

Abbreviations: Axial conductance (Kx), Central metaxylem (CMX), Introgression line (IL), Logarithm of the odds (LOD), Peripheral xylem (PX), Quantitative trait loci (QTL), Recombinant inbred lines (RILs), Terminal drought (TD), Well-watered (WW).

INTRODUCTION

Plant roots are the route for water and nutrients acquisition from the soil, and provide physical anchoring, photoassimilates storage, and interface with the rhizosphere. The root system architecture is responsive to spatiotemporal soil factors such as moisture and minerals availability, temperature and pH (Robbins & Dinneny, 2015). Root system characteristics including morphological and anatomical structure, carbon allocation plasticity, hydro- and gravitropism, and the rhizosheath, plays a crucial role in plants adaption and response to various environmental cues (Kitomi et al., 2020; Klein, Schneider, Perkins, Brown, & Lynch, 2020; Lynch, 2018; Rellan-Alvarez, Lobet, & Dinneny, 2016; Tracy et al., 2020; Uga et al., 2013). Better understanding of the root system genetic architecture can facilitate the development of new cultivars with ameliorate water-use efficiency for the projected climate change (Gupta, Rico-Medina, & Caño-Delgado, 2020; Palta & Turner, 2019; Preece & Peñuelas, 2020; Schneider & Lynch, 2020).

Water absorption from the soil to the transpiring leaf is mediated via complex anatomical-structural pathways, starting with the epidermis layer and the root hairs (tubular outgrowths of epidermal cells). Root hairs extend the absorbing surface by more than 50% and play an essential role in nutrient acquisition and water uptake from the soil (Carminati et al., 2017; Dolan, 2017). After entering the root, water moves either apoplastic (within parenchyma cell walls) or symplastic (crossing through cell membranes) route towards the root center. When water reaches the endodermis (outer layer) of the root cylinder, it encounters the casparian bands, which are suberin cell walls that force the water to move via the symplastic route until it is loaded into the xylem (Holbrook, 2018). Xylem is made up of hallow and dead cells- tracheae, which are positioned one on top of each other with a perforation plate between them, creating a long tube structure that continues through shoot and leaves.

Wheat (*Triticum* sp.) is a staple grain-crop, with an annual production of ~760 million tons worldwide. Wheat domestication and subsequent evolution under domestication involved a suite of complex genetic, morphological, anatomical, and physiological modifications (Abbo et al., 2014; Golan, Hendel, Méndez Espitia, Schwartz, & Peleg, 2018). Wild emmer wheat [*T. turgidum* ssp. *dicoccoides* (Körn.) Thell.], the direct allo-tetraploid (2n=4x=28; genome BBAA) progenitor of domesticated wheats, thrives across wide eco-geographic amplitude across the Fertile Crescent and offers ample allelic repertoire for agronomically important traits, including drought tolerance [e.g., Bacher et al., 2020; Golan et al., 2018; Peleg et al., 2005; Peleg et al., 2009]. During the

transition from natural habitat to anthropogenic agro-systems, ~10,500 years ago, many adaptive traits were lost or gradually eliminated from the domesticated germplasm.

The monocotyledonous wheat root system is composed of two types of roots: seminal roots (i.e. embryonic), and adventitious roots (i.e. crown or nodal) (Klepper, Belford, & Rickman, 1984). The seminal root system develops initially and consists the primary (or radicle) root and two pairs of seminal roots (#2-3 and #4-5) that develop at the scuttelar node of the embryonic hypocotyl (Percival, 1921). Seminal roots penetrate the soil earlier and deeper than the adventitious roots and usually remain active throughout the whole plant life cycle, and play a crucial role in absorbing water from deep soil layers (Locke & Clark, 1924; Watt, Magee, & McCully, 2008; Weaver, 1926). Seminal root xylem in wheat is usually patterned with one large metaxylem element in the center (CMX), and peripheral elements surrounding it in one or two rings. As the root develops, some of the peripheral elements can increase in size becoming similar to the initial CMX. In recent years, several studies on root system architecture uncovered the genetic basis of these traits, however, most studies focused on the geometric trait, such as root number, length, diameter and angle (Christopher et al., 2013; Golan et al., 2018; Hamada et al., 2012; Shorinola et al., 2019; Soriano & Alvaro, 2019; Voss-Fels, Snowdon, & Hickey, 2018), as the root anatomical traits remain largely unexplored.

Under the semi-arid Mediterranean climate, grain maturation period usually occurs under terminal drought. Therefore conserving a larger proportion of soil water moisture during the vegetative phase, is critical to support the subsequent grain filling. It has been suggested that restricting root hydraulic conductance can induce stomatal closure and minimize water loss (Vadez, Kholova, Medina, Kakkera, & Anderberg, 2014). In accordance, Richards and Passioura (1989) hypothesized that reducing wheat seminal roots xylem element size can decrease the hydraulic conductance and thereby decelerating early water-use. Here, we present evidence that lower Kx contributes supports sustainable grain yield under terminal drought. Further, we targeted Kx related morphological and anatomical seminal root traits and uncovered their underlining generic basis, using recombinant-inbred lines population, derived from a cross between durum wheat and wild emmer. Lastly, we show that introgression of major genomic region for Kx and CMX in modern durum wheat background can reshape its root hydraulic properties. The identified genomic regions may serve as a basis for future breeding efforts in developing wheat cultivars adapted to the projected climate change.

MATERIALS AND METHODS

Plant material

A mapping population of 150 F_8 recombinant inbred lines (RILs) was developed by single-seed descent from a cross between an elite durum wheat (♀) cultivar Svevo and the wild emmer wheat (♂) accession Zavitan, as was previously described (Avni et al., 2014). For QTL validation we used a set of introgression lines (ILs), derived from adaptive RILs [i.e. genetic composition of post-domestication alleles: reduce height (*Rht-B1*) and non-brittle spike (*Tdbtr*), that were backcrossed three times with Svevo follow by five generations of self, to generate BC_3F_5].

Seedlings growth conditions

Seedlings were grown using the 'cigar roll' method (Watt et al., 2013). Twelve uniform-size seeds of each line were placed on a moist germination paper (25 × 38 cm; Anchor Paper Co., St. Paul, MN, USA), about 2 cm apart, with the germ end facing down. The paper was covered with another sheet of moist germination paper rolled to a final diameter of 3 cm. The bases of the rolls were placed on a tray, with half-strength Hoagland solution, in a darkened growth chamber at a constant temperature of 16.5°C. The nutrient solution contained the following macro elements: KNO_3 (3mM), Ca $(NO_3)_2$ (2mM), KH_2PO_4 (1mM), $MgSO_4$ (0.4mM), and micronutrients: KCl (50μM), EDFS (30μM), H_3BO_3 (25μM), $ZnSO_4$ (2μM), $MnSO_4$ (2μM), H_2MoO_4 (0.75μM), $CuSO_4$ (0.5μM), pH=6.0. The root hair experiment was conducted after four days in the darkened growth chamber. The anatomical cuts and root length experiments were moved to a daily cycle of 10/14 hours of light and darkness at 16° and 24°C respectively, for three more days, in total 7 days after sowing. During the additional three days, the light intensity was 150-200 ($\mu mol\ s^{-1}\ m^{-1}$).

Characterization of seminal roots anatomical and physiological traits

Anatomical parameters of all experiments were taken using freehand sections as described previously (Zelko et al., 2012). Primary roots of seven-days old seedlings from each line (*n*=4) were cut at the root tip (1.5cm above the tip) and root base (1.5cm under the root-to-shoot junction) (Fig. 1).

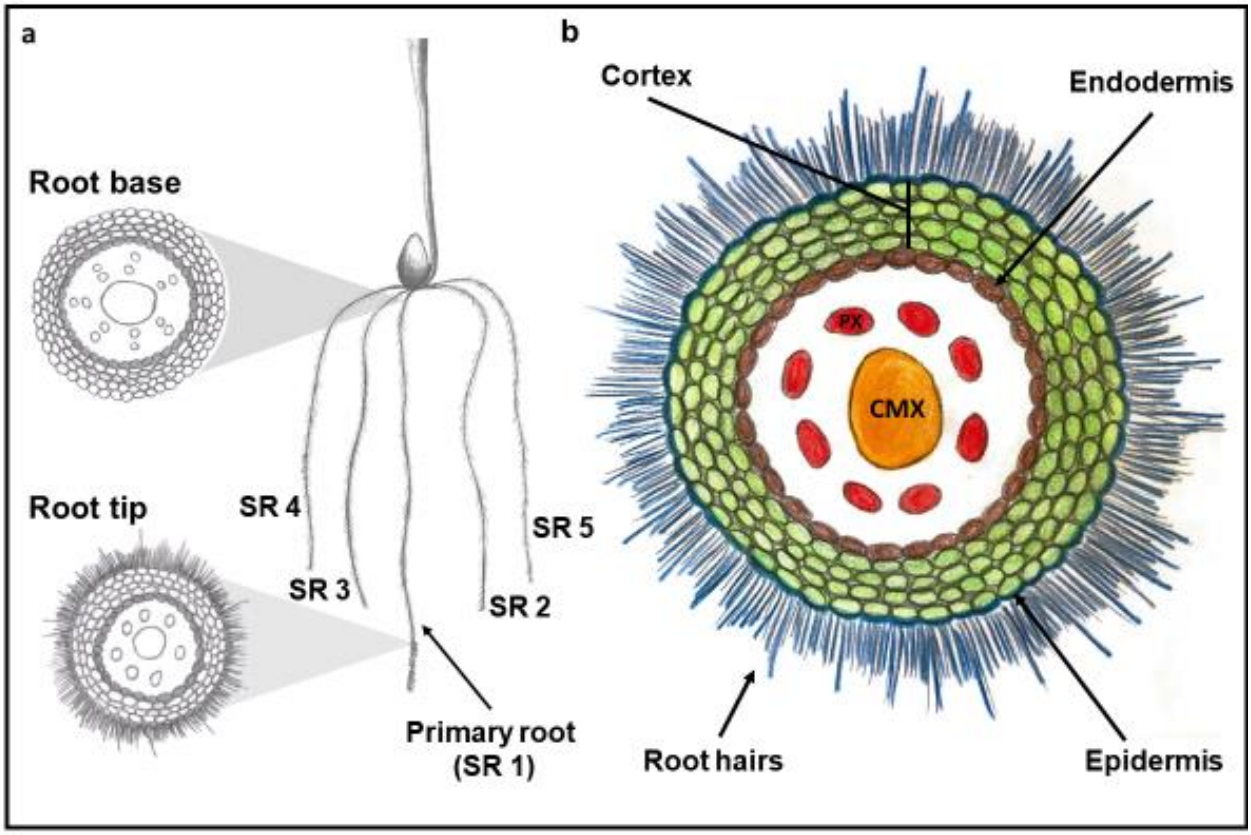

Figure 1. A schematic illustration of wheat seminal root apparatus and anatomical cross-section. (**a**) The primary seminal root (SR1), the two symmetric root pairs (SR2,3 and SR4,5) and location of root base and root tip cross-sections. (**b**) Root tip anatomy consists of central metaxylem (CMX), peripheral xylem (PX), endodermis, epidermis, cortical parenchyma (Cortex) and root hairs.

Each segment was embedded in agarose (5%) that was heated beforehand. After the agarose was hardened root sections were cut vertically using a razor, and stained with Toladine blue (0.0025% for 2 min). Sections were visualized using a Zeiss Axioplan equipped with an Axiocam 105 color camera (Zeiss, Germany). *Root diameter* (the diameter of the root circle), c*ylinder diameter* (the diameter of the root stele), *central metaxylem area* (CMX) and *peripheral xylem area* (PX, consisting of protoxylem and other xylem elements except for CMX) (see Fig. 1) were measured using Image J software (https://imagej.net/ImageJ_Ops). Transformation from diameter to area and *vice versa* were based on the assumption of perfectly cylindrical elements (Tyree & Ewers, 1991), for example in *CMX area to CMX diameter*.

Based on the measured traits we calculated the *total xylem area*, *xylem density in root*, *xylem density in a cylinder*, *relative CMX area* and *relative cylinder area* as presented in the following equations:

1. $Total\ xylem\ area = CMX\ area + PX\ area$
2. $Xylem\ density\ in\ root\ (\%) = \frac{Total\ xylem\ area}{Root\ area} \times 100$
3. $Xylem\ density\ in\ cylinder\ (\%) = \frac{Total\ xylem\ area}{Cylinder\ area} \times 100$
4. $Relative\ CMX\ area\ = \frac{Central\ xylem\ area}{Total\ xylem\ area}$
5. $Relative\ cylinder\ area = \frac{Cylinder\ area}{Root\ area}$

Axial conductivity (Kx) was calculated using modified Hagen–Poiseuille's equation for fluid flow through a bundle of perfectly cylindrical pipe as described previously (Tyree & Ewers, 1991):

$$K_X = \left(\frac{\pi\rho}{128\eta}\right)\sum_{i=1}^{n}(d_i^4)$$

wherek_x (kg s^{-1} m MPa^{-1}) is the hydraulic conductivity, ρ is the density of the fluid (for distilled water, 1,000 kg·m^{-3}), η is the dynamic viscosity of the fluid (for distilled water 10^{-9} MPa·s), d is the diameter (m) of the ith pipe, and n is the number of pipes.

Field-based characterization of Kx contribution to yield

Two genotypes with contrasting hydraulic properties: Svevo (high Kx) and IL82 (low Kx) were selected for this assay. A paired sample experimental design between the two genotypes with two irrigation regimes: well-watered (WW) and terminal drought stress (TD), was employed. Uniform seeds of Svevo and IL82 were sown in an insect-proof screen-house protected by a polyethylene top, during the winter of 2019–2020 at the experimental farm of The Hebrew University of Jerusalem in Rehovot, Israel (34°47′N, 31°54′E; 54 m above sea level). The soil at this location is brown-red degrading sandy loam (Rhodoxeralf) composed of 76% sand, 8% silt and 16% clay. Each plot consisted four rows, with 10 plants 10 cm apart where the circumference plants of each plot served as borders, resulting in a total of 16 plants examined for each plot. The field was treated with fungicides and pesticides to avoid development of fungal pathogens or insect pests, and was weeded manually once a week. Two irrigation regimes were applied via a drip system:

WW and TD treatments mimic the natural pattern of rainfall in the Eastern Mediterranean basin; water was applied during the winter months starting from planting (December 12, 2020) and ending on April 23. The wet treatment was irrigated twice a week, whereas the dry treatment was irrigated twice every other week. The seasonal water use, including irrigation and soil water depletion, was ~750 and ~250 mm for the WW and TD treatments, respectively.

Anatomical traits from field experiment have been taken with additional two steps: *i*) the top of the root system has been harvested with a small shovel (i.e., "mini-shovelomics"; Trachsel, Kaeppler, Brown, & Lynch, 2011), and *ii*) adventive roots had been removed manually to expose the seminal roots (Fig. S1). From this stage, the protocol for calculating anatomical traits was the same as mention above. At the end of the experiment, each plot was harvested, spikes were separated from the vegetative organs (stems and leaves) and both plant parts were oven-dried (80°C for 48 h) and weighed. Spikes were then trashed with laboratory seed thresher (Wintersteiger, LD-350), weighted and counted to obtain grain yield (GY) and thousand kernel weight (TKW). Relative grain yield was estimated for each genotype as the ratio between each plot under TD and the average performance under WW.

Morphological characterization of seminal roots traits

Whole root systems of seven-days old seedlings (Zadocks stage 10; Zadoks, Chang, & Konzak, 1974) were scanned in a flatbed scanner (Avision, FB5000), and *primary root length* was measured using the RootNav software (Pound et al., 2013). To analyze the root hair related traits, primary root of 4-days old seedling (Zadocks stage 09) was imaged above the elongation zone using a stereo microscope (SZX16, Olympus, Tokyo, Japan) equipped with a DP73 digital camera. *Root hair length* (RHL) was calculated as the average of 10 individual hairs in each photo using ImageJ software. *Root hair density* (RHD) was analyzed based on an index (range 1-6; Fig. S2) and scored by a panel of nine peoples (n=3).

QTL mapping correspondence hotspots and genomic dissection

A genetic linkage map of 2,110 cM long with an average distance of 0.92 cM was previously developed using the 90K iSelect SNP assay (Illumina) as described (Avni et al., 2014). The QTL analysis was performed with the MultiQTL software (ver. 4.6) using the general interval mapping for a RIL-selfing population, as previously described (Peleg et al., 2009). In brief, the entire

genome was screened for genetic linkage, using single-trait analysis (STA), follow application of multiple interval mapping (MIM), which incorporates into the model interfering effects of other QTL on separate chromosome to reduce the residual variation. The hypotheses that a single locus (H_1) or two linked loci (H_2) on the considered chromosome (chr.) have an effect on a given trait was compared against the null hypothesis (H_0) that the locus had no effect on that trait. Once the genetic model was chosen, 10,000 bootstrap samples were run to estimate the main parameters: locus effect, its chromosomal position, its logarithm of odds (LOD) score and the percentage of explained variance (PEV). For visualization, we used the QTL circos plot created with Circa (http://omgenomics.com/circa).

Correspondence between QTL of different traits was determined using the hypergeometric probability function, as described previously (Peleg et al., 2009):

$$P = \frac{\binom{l}{m}\binom{n-l}{s-m}}{\binom{n}{s}}$$

where *n* is the comparable number of intervals, *m* is the number of 'matches' (QTL of two traits with >50% overlap of their confidence intervals) declared between QTL, *l* is the total number of QTL found in the larger sample and *s* is the number of QTL found in the smaller sample. Hotspot genomic regions were designated as overlapping of at least three QTL. The genomic region size was considered from the QTL with the smallest standard deviation in the cluster and the other QTL that overlap with its boundaries.

Meta-analysis of overlaps between QTL detected in the current study and previously published information conducted on the GrainGenes genome browser (Blake et al., 2019), where the physical location of the QTL peak was used to locate a gene sequence on the Zavitan genome (Avni et al., 2017), and blast the sequence against Svevo genome (Maccaferri et al., 2019).

Statistical analyses of phenotypic data and visualization

Statistical analysis was done by JMP® ver. 15 statistical package (SAS Institute, Cary, NC, USA). Descriptive statistics are graphically presented in box plot: median value (horizontal short line), quartile range (25 and 75%) and data range (vertical long line), where t-test was applied between genotypes for all comparisons unless specified otherwise. Dunnett test was used to compare different ILs from their recurrent parent Svevo.

Visualization of phenotypic scaled density and morpho-anatomical phenotypic correlation matrix was done with R Studio (R_Core_Team, 2020). RStudio: integrated development for R. RStudio. Inc., Boston, MA), using "ggplot" and "corrplot" packages, respectively.

RESULTS

Lower axial conductance supports sustainable grain yield under terminal drought conditions

In order to test the contribution of wild emmer wheat alleles to axial conductance (Kx), we dissected a set of ten wild emmer introgression lines (ILs). In general, most ILs exhibited lower Kx as compared with their recurrent parent Svevo (42.08 *vs*. 50.94 kg s^{-1} m MPa^{-1}, Table S1, Fig. S3). Reduced size of seminal roots xylem element (i.e. decrease Kx) has been suggested to support wheat ability to cope with terminal drought (Richards & Passioura, 1989). Here we further test this hypothesis by field evaluation of two genotypes with contrasting Kx under Mediterranean semi-arid conditions. We selected IL82 which exhibited significantly lower Kx (33.37 *vs*. 50.94 kg s^{-1} m MPa^{-1}; $P<10^{-4}$) compared with Svevo (Fig. S3). Characterization of the two genotypes in the field conducted along three developmental phases which represent critical stages in wheat growth in the Mediterranean basin climate. During early growth stages the plants were grown under well-watered conditions, whereas terminal drought (TD) started to develop gradually during the transition from vegetative to reproductive stage. At seedling stage (Zadoks 11) IL82 exhibited 49% lower Kx compared to Svevo, which was maintained during the tillering (Zadoks 23-25) stage (53%) and at the end of the season (Zadoks 92) under well-watered (36%) (Fig. S4). Notably, the absolute values of Kx were reduced for both genotypes during the growing season. Under terminal drought, IL82 had significantly lower Kx (73.16 *vs*. 105.34 kg s^{-1} m MPa^{-1}), and higher GY (P=0.059; Table. S2) as expressed in its greater grain size (TKW) (Fig. 2a, b). It is worth noting that under TD, Svevo's grain yield reduction was ~two-fold larger compare to IL82 (Fig. 2c, d; Table. S2).

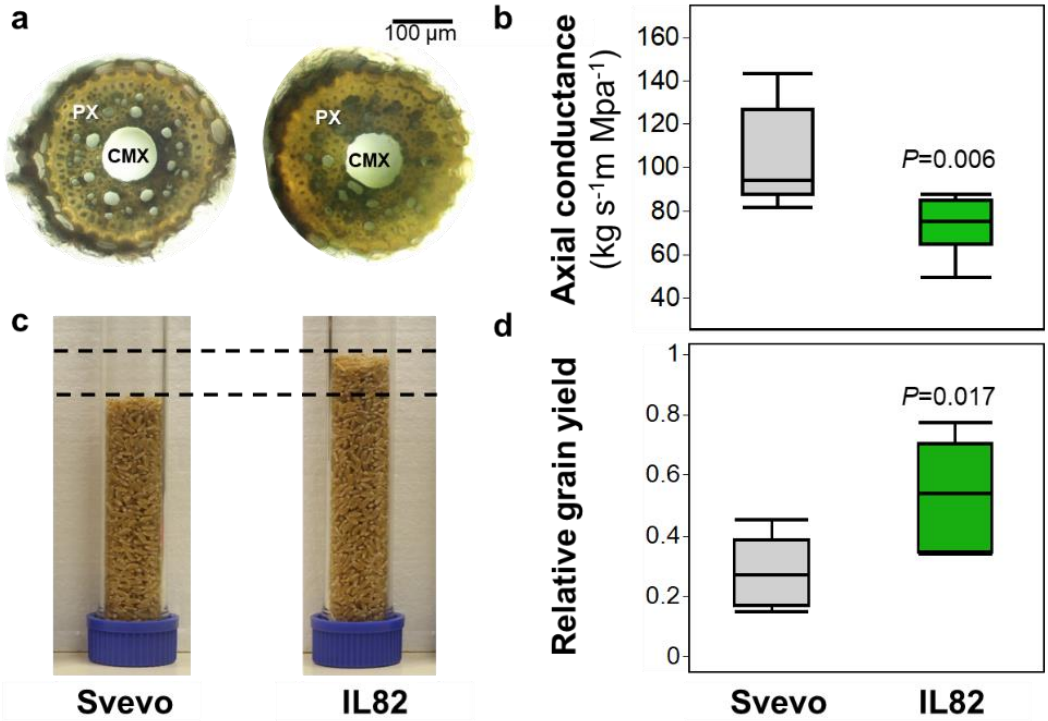

Figure 2. Field-based evaluation of primary seminal root Kx and grain yield under terminal drought conditions. (**a**) Root base anatomical cross-sections. Metaxylem (CMX) and peripheral xylem (PX) elements are indicated. (**b**) Axial conductance of Svevo and IL82 under terminal drought. (**c**) Comparison of two thousand grains between Svevo and IL82 under terminal drought. (**d**) Relative grain yield of Svevo and IL82 under terminal drought compared with well-watered conditions. Differences between genotypes were analyzed by t-test (n=5).

Phenotypic dissection of root morphological, anatomical and physiological traits

The contribution of lower Kx as the key trait supporting sustainable GY production under the Mediterranean climate motivated us to further dissect the genetic and physiological basis of Kx. We used a RIL population derived from a cross between wild emmer and durum wheat to determine the genetic architecture of various seminal root morphological and anatomical traits. Characterization of the population *primary root length* showed strong transgressive segregation (range 134-184 mm), with both parental lines exhibiting similar length (157.94 *vs*. 150.55 mm for Svevo and Zavitan, respectively) (Fig. 3a). Root hairs play important roles in nutrient and water uptake as well as interactions with the rhizosphere by increasing the root volume. In general, the two parents exhibited opposite trend in *root hair length* (RHL) and *root hair density* (RHD), while Svevo had higher RHL, Zavitan had higher RHD and vice versa. Notably, the population showed quantile frequency distribution with most RILs exhibiting similarly to the Zavitan parent (Fig. 3b, c).

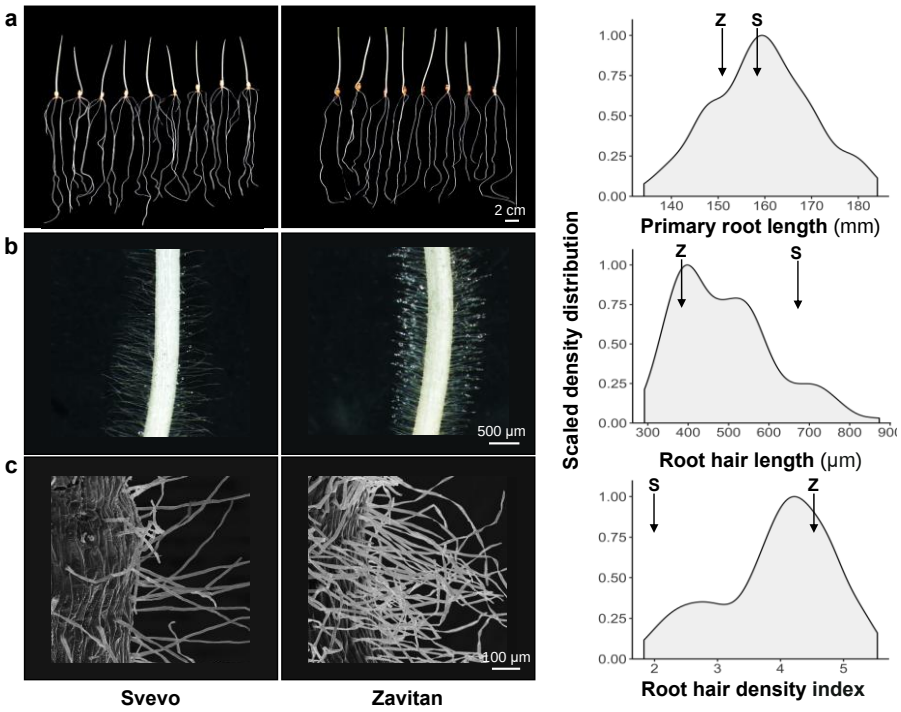

Figure 3. Phenotypic distribution of primary root morphological traits. A representative image of the two parental lines: Svevo and Zavitan, and density distribution of recombinant inbred lines population (Svevo × Zavitan) for (**a**) primary root length, (**b**) root hair length and (**c**) root hair density index. Values of the parental lines Svevo (S) and Zavitan (Z) indicate by arrows (*n*=3).

In order to characterize the anatomical structure of the seminal roots, we analyzed two developmental stages of xylem elements: root tip (i.e. middle differentiation process) and base (mature elements). Density distributions of root tip and base anatomical and physiological traits among the RILs presented in Figure 4. All variables exhibited normal distribution and most traits showed transgressive segregation. In general, the range of most measured traits (except root diameter) was higher in root base compared with root tip, with some level of overlapping (Fig. 4a-e). The two parental lines exhibited different behavior for root base and tip. While in some cases there was constant difference between the parents for both root tissues (root diameter, root cylinder diameter, total xylem area, relative cylinder area and xylem density in cylinder), in other cases the difference between the parents varied among tissues (PX area and relative CMX area). In two cases the parental lines showed opposite behavior (CMX diameter and Kx) (Fig. 4).

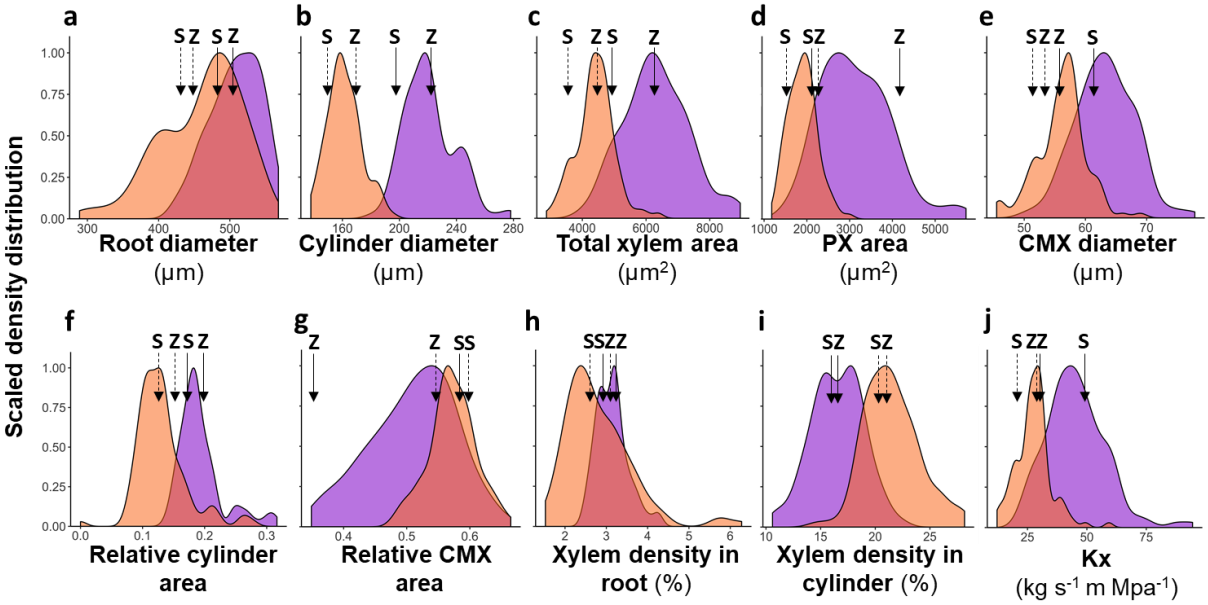

Figure 4. Density distribution of seminal roots anatomical and physiological traits: (**a**) root diameter (**b**) cylinder diameter, (**c**) total xylem area, (**d**) peripheral xylem (PX) area, (**e**) central metaxylem (CMX) diameter, (**f**) relative cylinder area, (**g**) relative CMX area, (**h**) xylem density in root, (**i**) xylem density in cylinder and (**j**) axial conductance (Kx), in 150 recombinant inbreed lines (Svevo × Zavitan) for root tip (orange) and root base (violet). Mean values of the parental lines, Svevo (S) and Zavitan (Z) are indicated by dashed (root tip) and solid (root base) arrows.

Inter-relationships between anatomical, morphological and physiological root traits

To understand the relationships between the various seminal root morphological, anatomical and physiological traits, and test the effect of the developmental stages between root tip and base, we performed correlation analysis. The root morphological traits (primary root length, RHD, RHL) were not associated with either root base or tip anatomical traits, neither with themselves (Fig. 5; Table S3). Correlation between anatomical and physiological traits in root base and root tip showed that while some traits maintained similar pattern [Kx (r=0.52), total xylem area (r=0.65), and xylem density (r=0.69)] others had different behavior [root diameter (r=0.16), relative CMX area (r=0.20), and xylem density in root (r=0.20)] (Fig. 5; Table S4). Base Kx was positively correlated with the anatomical traits in root base: CMX diameter (r=0.93, $P=1\times10^{-4}$), total xylem area (r=0.76, $P=1\times10^{-4}$) and root diameter (r=0.53, $P=1\times10^{-4}$). Tip Kx showed similar pattern, except for root diameter (Fig. 5; Table. S3). While Kx is a consequence of total xylem area (Hagen-Poiseuille's equation), the larger elements can have strong effect on the outcome value. Notably, relative CMX area showed no correlation with Kx (r=0.1 and 0.2 for root base and root tip, respectively; Table S3).

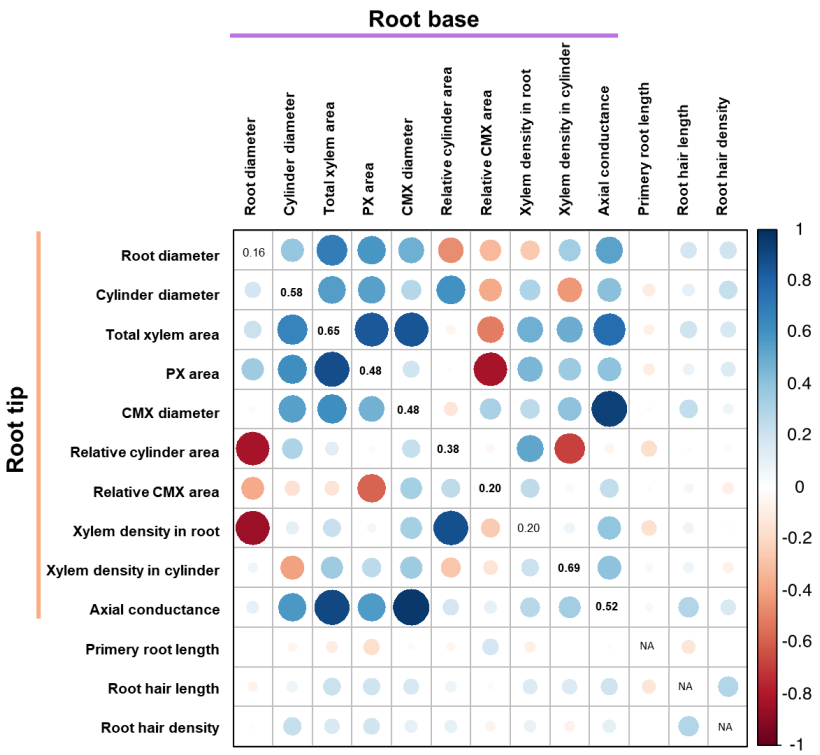

Figure 5. Pearson correlation matrix between the seminal roots morphological, anatomical and physiological traits: root diameter, cylinder diameter, total xylem area, peripheral xylem (PX) area, central metaxylem (CMX) diameter, relative cylinder area, relative CMX area, xylem density in root, xylem density in cylinder, axial conductivity (Kx), primary root length, root hair length, root hair density. The upper and lower triangle represents the root base and root tip traits, respectively. The diagonal values represent correlation between root base and root tip, whereas in primary root length, root hair length and root tip only one observation had been taken. Bold values represent statistical significance ($P \leq 0.05$). Colors indicate the level of correlation (r) from positive correlation (blue) to negative (red). Circle size indicates the level of significance.

Genetic architecture of seminal root morphological, anatomical and physiological traits

To better understand the genetic basis of the seminal roots morphological, anatomical and physiological traits, we conducted QTL analysis, which resulted in 75 QTL. For each trait, we detected between one QTL (tip root diameter and tip relative CMX area) to 8 QTL (primary root length and base PX area), with two traits (tip xylem density in cylinder and tip Kx) without detected QTL. LOD score ranged from 2.68 (base xylem density in root) to 10.72 (primary root length), explaining from 14% (tip relative CMX area) to 77.6% (primary root length) of the phenotypic variance. For all QTL we considered the higher value as additive. In general, for most QTL, the Svevo allele conferred higher values (42 *vs.* 33), with 41 QTL located on the A sub-genome and 34 on the B sub-genome (Tables 1, S5; Fig. 6). Genetic correlations between traits resulted in several significant associations: base root diameter and tip PX area (P=0.01), base xylem density

in cylinder with tip PX area (P=0.01), tip relative cylinder area and tip xylem density in root ($P<10^{-4}$), and primary root length and base CMX diameter (on adage of significance, P=0.076) (Table S6).

Table 1. Summary of quantitative trait loci (QTL) detected in tetraploid wheat (Svevo × Zavitan RILs population) associated with seminal roots morphological, anatomical, and physiological traits.

Trait	#QTL	LOD[a]	PEV[b]	Svevo[c]	Zavitan
Primary root length	8	6.78-10.72	77.6	5	3
Root hair length	5	4.15-5.07	20.8	4	1
Root hairs density	2	3.45-3.60	39.4	1	1
Total	**15**			**10**	**5**

	Root Base					Root tip				
Trait	**#QTL**	**LOD**	**PEV**	**Svevo**	**Zavitan**	**#QTL**	**LOD**	**PEV**	**Svevo**	**Zavitan**
Root diameter	2	2.71-4.45	24.3	1	1	1	3.56	16.2	0	1
Cylinder diameter	2	3.39-4.23	24.3	1	1	4	4.58-6.49	58.2	1	3
Total xylem area	4	4.37-5.75	24.8	2	2	5	3.75-6.55	58.2	2	3
Peripheral xylem	8	3.92-7.79	35.3	4	4	3	3.63-4.73	38.7	2	1
Central metaxylem diameter	5	3.12-8.50	67.8	4	1	2	5.63	37.0	1	1
Relative cylinder area	4	3.83-9.34	51.8	2	2	2	6.50	43.9	1	1
Relative central metaxylem area	7	4.60-9.91	58.4	5	2	1	3.16	14.0	0	1
Xylem density in root	2	2.68-3.00	68.0	1	1	2	6.75	42.5	1	1
Xylem density in cylinder	2	3.01-4.07	23.8	2	0	n.d.				
Axial conductance	4	6.11-6.13	19.7	2	2	n.d.				
Total	**40**			**24**	**16**	**20**			**8**	**12**

[a]. LOD scores that were found significant when comparing hypotheses H_1 (there is a QTL in the chromosome) *vs*. H_0 (no effect of the chromosome on the trait), using 1000-permutation test (Churchill & Doerge, 1994).
[b]. Proportion of explained variance of the trait.
[c]. The allele contributing higher value of each trait.
n.d., not detected.

Major genomic regions associated with several overlapping QTL, i.e. hotspots, can indicate either cluster of several genes with different function or major gene with pleiotropic effect. We targeted two hotspots with overlapping QTL (additive effect marked for the higher allele, Svevo and Zavitan). On chromosome 5A (564,800,028-672,857,031bp), primary root length (Z), RHD (S), base relative CMX area (Z), base PX area (S), base cylinder diameter (S). On chromosome 6A (105.254 ±19.51*cM*) consist five QTL: base root diameter (S), base relative cylinder area (Z), base xylem density in cylinder (S), base PX area (S) and tip PX area (S) (Fig. S5)

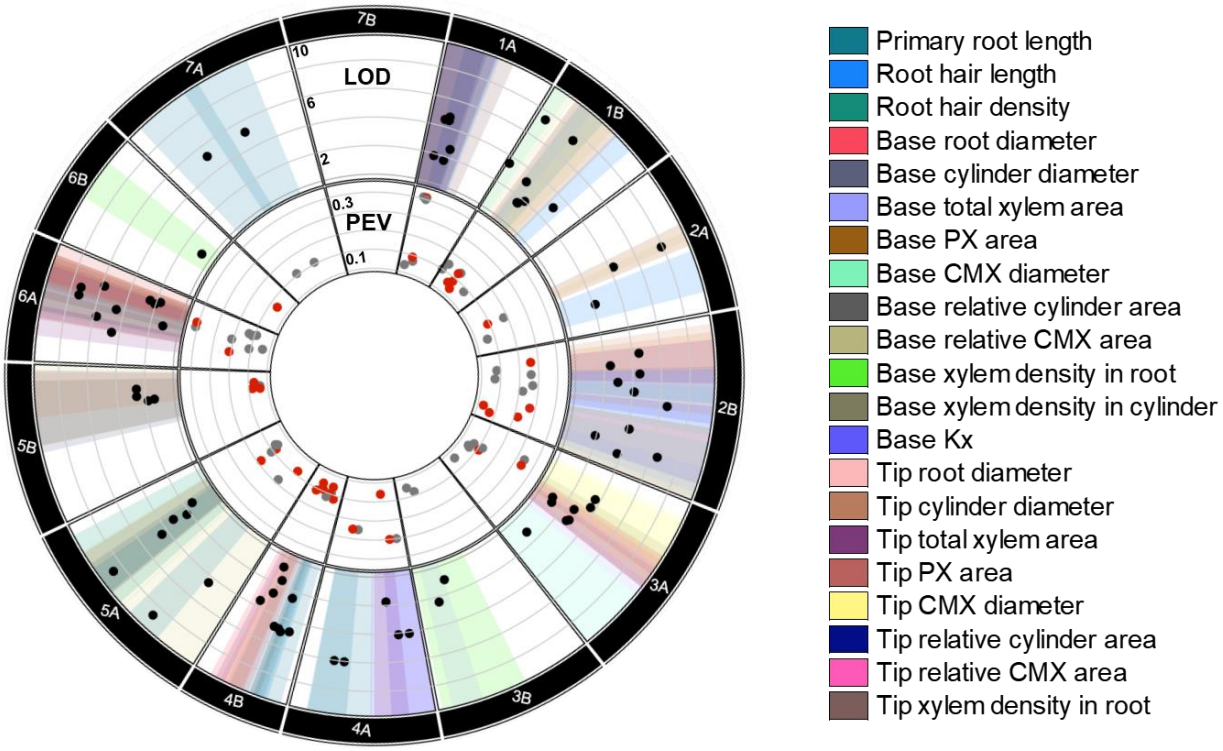

Figure 6. Quantitative trait loci (QTL) associated with 21 seminal root traits in recombinant inbred lines (RILs) of the cross between Svevo and Zavitan. Traits were analyzed in the root tip and based for *morphological*: primary root length, root hair length and root hair density; *anatomical*: root diameter, cylinder diameter, total xylem area, peripheral xylem (PX) area, central metaxylem (CMX) diameter, relative cylinder area, relative CMX area, xylem density in root and xylem density in cylinder. *Physiological*: axial conductance (Kx). Circos diagram showing, from the outer to inner tracks, the wheat chromosomes, QTL for specific traits and their positions, LOD score (black markers), percentage of explained variance (PEV) where Svevo (grey) and Zavitan (red) additive contribution are marked.

Validation of ancestral axial conductance related alleles

Zavitan accession was collected from natural habitat with shallow brown basaltic soil type, which has high soil moisture fluctuation (Peleg et al., 2008). Thus, we targeted wild alleles that could be important for reshaping the root architecture to cope with fluctuating soil moisture for further analysis. To validate the major root base QTL affecting Kx, and CMX diameter, we used wild emmer wheat Zavitan introgression lines in background of elite durum wheat Svevo. Two QTL conferring base Kx on chrs. 2B (Svevo) and 4A (Zavitan) were tested using IL with opposite genetic composition: IL108 (Zavitan and Svevo) and IL95 (Svevo and Zavitan, respectively). Overall, our results validated the QTL composition, with IL95 exhibiting significantly higher base Kx (54.75 *vs*. 44.49) compared with Svevo, whereas IL108 had significantly lower base Kx (34.77) (Fig. 7).

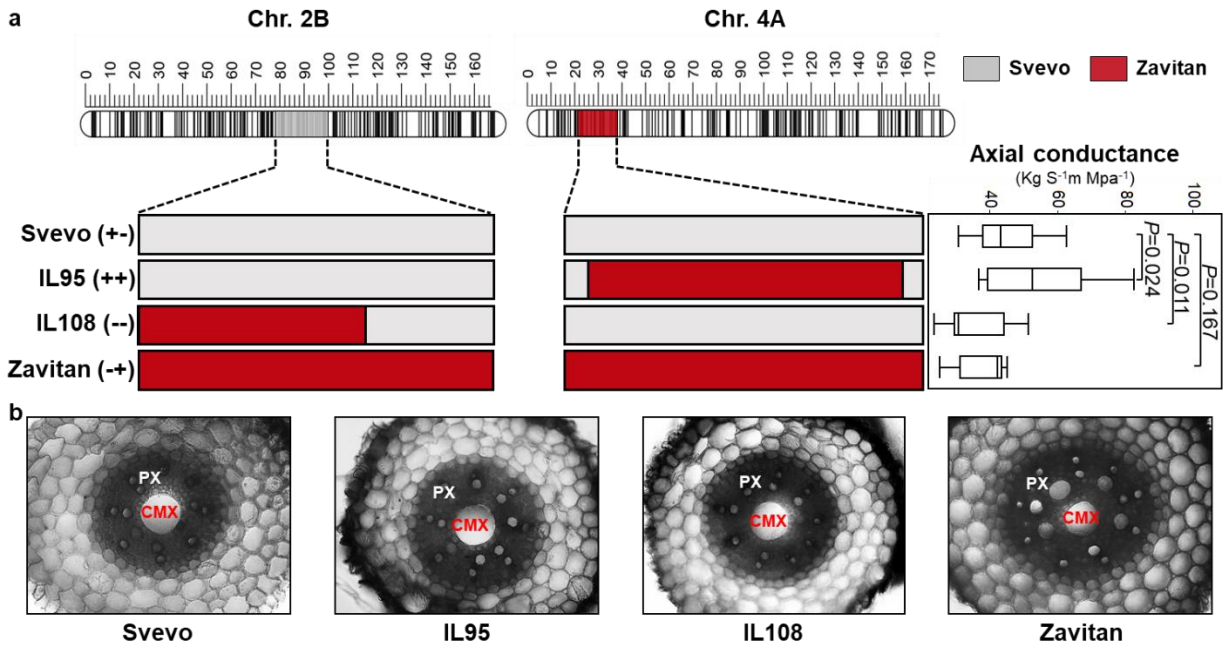

Figure 7. Validation of QTL for seminal root axial conductance (Kx). (**a**) Graphical genotyping of the two parental lines (Svevo and Zavitan) and two wild emmer introgression lines (IL108 and IL95) harboring Kx QTL on chromosomes 2B and 4A, respectively. The Box plot represents each genotype Kx and comparison to the recurrent parent Svevo according to Dunnett test (*n*=8). (**b**) A represented image of seminal root base anatomical cross-section of each genotype. The central metaxylem (CMX) and peripheral xylem (PX) are marked.

We validated two base CMX diameter QTL (on chrs. 1B and 6A), where Svevo contributed the adaptive allele, using IL100 and IL64 that harbor the Zavitan allele, respectively. Both ILs as well as Zavitan, exhibited significantly lower (~12%) CMX diameter compared to Svevo (Fig. 7). Notably, while CMX diameter has a pivotal role determining Kx (as expressed in Hagen-Poiseuille's equation), most CMX diameter QTL did not overlap Kx QTL.

DISCUSSION

Enhance tolerance to water stress through breeding is essential for maintaining production under the projected climate change (Anderson, Bayer, & Edwards, 2020). While genetic dissection of various above-ground traits has greatly improved our knowledge (Salvi & Tuberosa, 2015), in recent years more emphasis is given to the hidden half of the belowground root system. Most of these studies focus on the root system architecture morphology [i.e., root length, density, and angle (Lynch, 2019; Voss-Fels et al., 2018)], aiming to discover QTL with potential to improve water

and nutrient acquisition under suboptimal environments. However, the genetic basis of root anatomical and physiological traits where less studied, presumably due to their highly quantitative nature and small effect (Schneider & Lynch, 2020).

Form lab- to field-based high-throughput root traits phenotyping

The "out-of-sight" nature and extreme phenotypic plasticity of roots under native field conditions (due to dynamic responses to varying water, nutrient and environmental cues) and the limited availability of high-throughput phenotyping tools, inhibited functional genetic studies of root architecture and especially anatomical and physiological traits (Atkinson, Pound, Bennett, & Wells, 2019; Watt et al., 2020). Moreover, the opaque nature of the soil further increases the complexity of *in-situ* phenotyping of root systems. While controlled (i.e. hydroponic) root phenotyping was not always good predictor of the field situation (Rich et al., 2020), Alahmad et al. (2019) showed that root angle phenotyping in the lab was consistent with the expression in the field. Likewise, seminal root number phenotypes observed in hydroponic conditions are transferrable to soil conditions, especially during the vegetative phase (Golan et al., 2018; Richard et al., 2015; Watt et al., 2013).

For this study, an important question was to determine if the young seedling assay for phenotypic differences can be observed for longer duration in the field? Our wide screening of young seedlings using the cigar-roll method (i.e. on germination paper) in control conditions enabled us to identify genotypes with contrasting Kx (Svevo and IL82). Further field-based analysis revealed that although the absolute values were larger compared with the lab experiment, a similar trend of ~50% difference between the genotypes was maintained throughout development (Figs. 2, S3, S4). Thus, the phenotypic approach developed for the current study can represent the field performance in terms of axial conductance and related anatomical traits.

Root morphological traits are independent from other root properties

Under the semi-arid Mediterranean climate, soil moisture in the upper layer is limited and young seedlings are exposed to frequent events of dehydration. Recently, we showed that during wheat evolution under domestication, the number of seminal roots increased (from 3 to 5) due to activation of two root meristems (Golan et al., 2018). While one can expect that the difference in number of seminal roots will affect morphological and anatomical root traits, surprisingly, we

could not find any QTL overlaps between seminal root number and these traits. Fast development of seminal roots is important for reaching deeper soil layers to avoid the dehydration associated with the erratic rain distribution of the Mediterranean basin. Eight QTL associated with primary root (SR1; Fig. 1) length were found in the current study (Table S5), explaining most (76%) of the phenotypic variance. Since both parental lines have full genome sequence, we were able to test genetic overlaps with previous studies and focused on three genomic regions on chrs. 4A, 4B and 7A (Maccaferri et al., 2016), whereas the other five QTL (chrs. 4A, 4B, 5A, 5B, and 7A) are novel.

The proliferation of root hairs along major root axes has been implicated in a range of processes including, enhanced water uptake and nutrient acquisition, root-microbial signal exchange, allelochemical release and plant anchoring (Carminati et al., 2017; Holz, Zarebanadkouki, Kuzyakov, Pausch, & Carminati, 2018). While all these processes associated with the contribution of root hair to extending the effective radius surface area of the root, existing results on their function not fully understood. Moreover, quantification of root hairs features is challenging as the trait is highly affected by environmental conditions (Salazar-Henao, Vélez-Bermúdez, & Schmidt, 2016). As consequence, the genetic basis of root hairs was less studied, and the limited available research tested only root hair length (Horn, Wingen, Snape, & Dolan, 2016; Liu et al., 2017).

Here we dissect root hair characteristics into length (RHL) and density (RHD) in attempt to represent the complexity of the tissue. The different contribution of root hair length and density is exemplified in the comparison between the two parental lines of our mapping population. While the wild parental (Zavitan) had short root hairs compared to the domesticated parent (Svevo), its density was much higher (Fig. 3b, c). In general, our genetic analysis resulted in identification of five QTL for root hair length and two QTL for root hair density (Fig. 6; Table. S5). Genetic analysis of root hair length in hexaploid populations [bread wheat (Horn et al., 2016) and spelt wheat (Okano et al., 2020)] resulted in 4 and 1 QTL, respectively. Only one of these QTL (chr. 2A) co-localized with the five root hair length QTL found in the current study for tetraploid wheat, which further emphasizes the potential of finding new alleles in wild wheat germplasm. Genetic characterization of root hair density in wheat or other grasses remains unexplored. It is worth noting that in contrast with our initial hypothesis, low correlation was found between root hair traits and other anatomical traits ($r<0.3$; Fig. 5). Thus, it is yet to be discovered how root hair length and density interact with other root trait and their collective effect on water uptake.

Genetic architecture of xylem elements suggests independent control among young and mature root tissue

Xylem tracheary elements have a unique life cycle; from cell differentiation in the root tip to rapidly programmed cell death as they reach their full function state (Fukuda, 1997), which makes it difficult to track precisely each developmental stage. To study the root anatomical traits, we analyze the root tip, which represents the differentiating stage, and the root base, which represents mature cells. In accordance, we found that cylinder diameter and xylem elements increased from tip tissue to the root base as indicated by the significant positive correlation between tissues (Figs. 4b-e, 5). Generally, we were able to detect more QTL for anatomical traits in the root base compared with tip, and surprisingly most QTL did not co-localized, which suggests distinct genetic regulation of xylem development on a spatial scale (Fig. 6; Table. S5).

In temperate cereal roots, axial conductance (Kx) was found to be low in the tip differentiation zone and steady along the mature root tissue (Bramley, Turner, Turner, & Tyerman, 2009; Knipfer & Fricke, 2010). While we were able to detect QTL associated with the CMX and PX, no QTL for Kx in root were identified (Table 1; Fig. 6). Notably, Kx in root tip was strongly correlated with base (r=0.52, P<0.0001; Table S4). This change in the genetic regulation of the trait may be consequence of the fact that xylem elements reach maturity after 96 h (Fukuda, 1997), and during this stage, there is strong environmental effect as expressed in higher coefficient of variance (CV=27, CV=7.2 and CV=17.6 for Kx, CMX and PX, respectively). Hence, we decided to focus on the root base Kx as the representative of root potential conductance. It is important to mention that while one can expect maintenance of mature xylem elements size (dead cells) along the whole plant life cycle, in the field we found a decrease in Kx throughout the season (Fig. S4). It is an open question how xylem elements dimensions alter throughout root development and growth.

Reshaping root hydraulics via axial conductance QTL

Lower root Kx was identified as a key trait supporting sustainable grain yield under TD, subsequent of reduced water uptake during the early stages of growth (Richards & Passioura, 1989). Likewise, our field trial resulted in 9% yield advantage for IL82 with lower Kx (30%) under TD (Fig. 2; Table S2). In contrast to Richards and Passioura's (1989) findings, our results

suggest that IL82 had lower yield under WW conditions likely due to a yield penalty associated with lower Kx (Table S2). Although Passioura's concept was introduced ~40 years ago (Passioura, 1983), and repeatedly discussed in the literature (e.g., Berger, Palta, & Vadez, 2016; Blum, 2009; Richards, Rebetzke, Condon, & van Herwaarden, 2002), the genetic basis of Kx was not studied yet. Here we integrated new high-throughput root anatomical cross-section pipeline together with population derived from cross between wild and domesticated wheat to determine the genetic basis of root Kx. Four novel genomic regions associate with root Kx were identified, which explain most of the phenotypic variance (62%). Meta-analysis of these genomic regions exposed co-localization with QTL for grain yield on chr. 2B in population of durum wheat × wild emmer, under water-limited (Peleg et al., 2009) (Table S7). Notably, both alleles are derived from the wild emmer (Zavitan reduce Kx and G18-16 increased yield, respectively).

Wild emmer has evolved over long evolutionary history under the fluctuation precipitation of the Mediterranean basin and accumulated ample genetic diversity for drought adaptations (e.g., Golan et al., 2018; Peleg et al., 2009). Under such conditions, narrow xylem elements can contribute to the natural population survival and seed set. Introgression of wild Kx allele (Zavitan) into Svevo background further validates the potential of wild alleles for redesigning seminal root anatomy and hydraulic properties of modern wheat with increased resilience (Fig. 7). However, root hydraulics is a complex trait associated not only with Kx but also with radial conductivity and root architectural traits that were not examined in the current study. Since roots are highly plastic, it remains to be determined, how altering one specific allele could impact the compensating response among other traits.

Xylem elements spatial distribution affect its hydraulic properties

Under water-limiting environments, xylem vessel diameter and distribution affect plant resistance to embolisms (Lucas et al., 2013). Anatomical characterization of the two parental lines revealed unique xylem vessels distribution of Zavitan's, with narrow CMX and larger PX (Fig. 7b). Prompted by this observation, we integrated a new index of relative CMX area, which represents the ratio of CMX from the total xylem area. Notably, Zavitan expressed the lowest values compared to the whole RILs population (Fig. 4g). Genotypes which have similar total xylem area differ dramatically in the relative CMX area (Fig. S7). Moreover, most QTL associated with CMX

and PX did not show genomic co-localization, which suggests that there is a possibility to break the compensating association between both traits.

From hydraulic perspective, this ratio between CMX and PX could also play a role in reducing the risk for cavitation under drought. Cavitation occurs when the tension in the vessels increases to a point of air bubbles formation and water column break. This phenomenon may occur due to expulsion to periods of severe drought and can result in loss of function of the whole vessel. It is suggested that wider vessels are at higher risk to cavitation (Melvin, Stephen, & Hervè, 1994; Strock, Burridge, Niemiec, Brown, & Lynch, 2020), hence plants with lower CMX area may be less susceptible to cavitation. Moreover, even in case of CMX failure, plants with larger PX (as found in the wild accession Zavitan) have the potential to meet transpiration demand. It is worth noting that IL82, which had higher GY under TD and low Kx, exhibited also has significantly lower relative CMX area compared with Svevo (P=0.002). Collectively, our results suggest that the relative CMX area should be considered a target trait for breeding drought resilience cultivars.

Conclusion and future perspective

Here we tested the hypothesis that under the terminal drought conditions associated with Mediterranean basin, smaller xylem vassals decrease water-use, thus supporting more water residuals for the critical phase of grain filling (Passioura, 1972). A field-based characterization further supports the key role of lower Kx in promoting sustainable grain production under terminal drought conditions. We harnessed the wide genetic diversity of wild emmer wheat to uncover the genetic basis of Kx and associated morphological, anatomical, and physiological seminal root traits. To the best of our knowledge, this is the first report on QTL associated with seminal roots anatomical and physiological traits in wheat. Our results help shed new light on the structural and functional anatomy of seminal roots and their association with yield sustainability under suboptimal environments. Integration of the identified wild alleles into future breeding programs may facilitate the optimization of seminal root hydraulic properties and should be considered while shaping the development of new wheat (and other cereals) cultivars for the projected climate change environments.

Acknowledgment

We thank members of the Peleg lab for helpful comments during the preparation of this work. We would like to thank N. Teboul for her assistance with the fine mapping, Dr. R. Hayouka for her technical support with the phenotyping experiments and L. Shemesh for drawing the seminal roots illustration. This study was partially supported by the Israel Ministry of Agriculture and Rural Development (grants # 20-10-0066; 12-01-0005), and the U.S. Agency for International Development Middle East Research and Cooperation (grant # M34-037).

Author contributions

EH, HB, AO, NS and ZP designed the experiments. EH, HB and AO conducted the phenotyping experiments. EH, HB and ZP conducted the genetic analyses. EH and HB conducted and analyzed the field experiments. EH, HB, HW and ZP wrote the paper. All authors have read and approved the manuscript.

References

Abbo, S., Pinhasi van-Oss, R., Gopher, A., Saranga, Y., Ofner, I., & Peleg, Z. (2014). Plant domestication versus crop evolution: a conceptual framework for cereals and grain legumes. *Trends in Plant Science, 19*, 351-360.

Alahmad, S., El Hassouni, K., Bassi, F. M., Dinglasan, E., Youssef, C., Quarry, G., . . . Hickey, L. T. (2019). A major root architecture QTL responding to water limitation in durum wheat. *Frontiers in Plant Science, 10*, 436.

Anderson, R., Bayer, P. E., & Edwards, D. (2020). Climate change and the need for agricultural adaptation. *Current Opinion in Plant Biology, 56*, 197-202.

Atkinson, J. A., Pound, M. P., Bennett, M. J., & Wells, D. M. (2019). Uncovering the hidden half of plants using new advances in root phenotyping. *Current Opinion in Biotechnology, 55*, 1-8.

Avni, R., Nave, M., Barad, O., Baruch, K., Twardziok, S. O., Gundlach, H., . . . Distelfeld, A. (2017). Wild emmer genome architecture and diversity elucidate wheat evolution and domestication. *Science, 357*, 93-97.

Avni, R., Nave, M., Eilam, T., Sela, H., Alekperov, C., Peleg, Z., . . . Distelfeld, A. (2014). Ultra-dense genetic map of durum wheat × wild emmer wheat developed using the 90K iSelect SNP genotyping assay. *Molecular Breeding, 34*, 1549-1562.

Bacher, H., Zhu, F., Gao, T., Liu, K., Dhatt, B. K., Awada, T., . . . Walia, H. (2020). Wild emmer introgressions alter root-to-shoot growth dynamics under water stress. *BioRxiv*, 2020.2006.2017.157461.

Blake, V. C., Woodhouse, M. R., Lazo, G. R., Odell, S. G., Wight, C. P., Tinker, N. A., . . . Sen, T. Z. (2019). GrainGenes: centralized small grain resources and digital platform for geneticists and breeders. *Database, 2019*, baz065

Bramley, H., Turner, N. C., Turner, D. W., & Tyerman, S. D. (2009). Roles of morphology, anatomy, and aquaporins in determining contrasting hydraulic behavior of roots. *Plant Physiology, 150*, 348-364.

Carminati, A., Passioura, J. B., Zarebanadkouki, M., Ahmed, M. A., Ryan, P. R., Watt, M., & Delhaize, E. (2017). Root hairs enable high transpiration rates in drying soils. *New Phytologist, 216*, 771-781.

Christopher, J., Christopher, M., Jennings, R., Jones, S., Fletcher, S., Borrell, A., . . . Hammer, G. (2013). QTL for root angle and number in a population developed from bread wheats (*Triticum*

aestivum) with contrasting adaptation to water-limited environments. *Theoretical and Applied Genetics, 126*, 1563-1574.

Churchill, G. A., & Doerge, R. W. (1994). Empirical threshold values for quantitative trait mapping. *Genetics, 138*, 963-971.

Dolan, L. (2017). Root hair development in grasses and cereals (Poaceae). *Current Opinion in Genetics & Development, 45*, 76-81.

Fukuda, K. (1997). Physiological process of the symptom development and resistance mechanism in pine wilt disease. *Journal of Forest Research, 2*, 171-181.

Golan, G., Hendel, E., Méndez Espitia, G. E., Schwartz, N., & Peleg, Z. (2018). Activation of seminal root primordia during wheat domestication reveals underlying mechanisms of plant resilience. *Plant, Cell & Environment, 41*, 755-766.

Gupta, A., Rico-Medina, A., & Caño-Delgado, A. I. (2020). The physiology of plant responses to drought. *Science, 368*, 266-269.

Hamada, A., Nitta, M., Nasuda, S., Kato, K., Fujita, M., Matsunaka, H., & Okumoto, Y. (2012). Novel QTLs for growth angle of seminal roots in wheat (*Triticum aestivum* L.). *Plant and Soil, 354*, 395-405.

Holbrook, N. M. (2018). Water Balance of Plants. In: L. Taiz, E. Zeiger, I. M. Møller, & A. S. Murphy (Eds.), *Plant physiology and development 6th Edition*: Sinauer Associates is an imprint of Oxford University Press.

Holz, M., Zarebanadkouki, M., Kuzyakov, Y., Pausch, J., & Carminati, A. (2018). Root hairs increase rhizosphere extension and carbon input to soil. *Annals of Botany, 121*, 61-69.

Horn, R., Wingen, L. U., Snape, J. W., & Dolan, L. (2016). Mapping of quantitative trait loci for root hair length in wheat identifies loci that co-locate with loci for yield components. *Journal of Experimental Botany, 67*, 4535-4543.

Kitomi, Y., Hanzawa, E., Kuya, N., Inoue, H., Hara, N., Kawai, S., . . . Uga, Y. (2020). Root angle modifications by the *DRO1* homolog improve rice yields in saline paddy fields. *Proceedings of the National Academy of Sciences USA, 117*, 21242-21250.

Klein, S. P., Schneider, H. M., Perkins, A. C., Brown, K. M., & Lynch, J. P. (2020). Multiple integrated root phenotypes are associated with improved drought tolerance. *Plant Physiology, 183*, 1011-1025.

Klepper, B., Belford, R. K., & Rickman, R. W. (1984). Root and shoot development in winter wheat. *Agronomy Journal, 76*, 117-122.

Knipfer, T., & Fricke, W. (2010). Water uptake by seminal and adventitious roots in relation to whole-plant water flow in barley (*Hordeum vulgare* L.). *Journal of Experimental Botany, 62*, 717-733.

Liu, M., Rathjen, T., Weligama, K., Forrest, K., Hayden, M., & Delhaize, E. (2017). Analysis of aneuploid lines of bread wheat to map chromosomal locations of genes controlling root hair length. *Annals of Botany, 119*, 1333-1341.

Locke, L. F., & Clark, J. A. (1924). Development of wheat plants from seminal roots. *Agronomy Journal, 16*, 261-268.

Lucas, W. J., Groover, A., Lichtenberger, R., Furuta, K., Yadav, S.-R., Helariutta, Y., . . . Kachroo, P. (2013). The plant vascular system: Evolution, development and functions. *Journal of Integrative Plant Biology, 55*, 294-388.

Lynch, J. P. (2018). Rightsizing root phenotypes for drought resistance. *Journal of Experimental Botany, 69*, 3279-3292.

Lynch, J. P. (2019). Root phenotypes for improved nutrient capture: an underexploited opportunity for global agriculture. *New Phytologist, 223*, 548-564.

Maccaferri, M., El-Feki, W., Nazemi, G., Salvi, S., Canè, M. A., Colalongo, M. C., . . . Tuberosa, R. (2016). Prioritizing quantitative trait loci for root system architecture in tetraploid wheat. *Journal of Experimental Botany, 67*, 1161-1178.

Maccaferri, M., Harris, N. S., Twardziok, S. O., Pasam, R. K., Gundlach, H., Spannagl, M., . . . Cattivelli, L. (2019). Durum wheat genome highlights past domestication signatures and future improvement targets. *Nature Genetics*. *51*, 885–895.

Melvin, T. T., Stephen, D. D., & Hervè, C. (1994). Biophysical perspectives of xylem evolution: is there a tradeoff of hydraulic efficiency for vulnerability to dysfunction? *IAWA Journal, 15*, 335-360.

Okano, N., Goto, R., Kato, T., Saisho, D., Kato, K., Miura, H., . . . Onishi, K. (2020). Spanish spelt is unique germplasm for improvement of root hair length in hexaploid wheat. *Plant and Soil, 452*, 171-184.

Palta, J. A., & Turner, N. C. (2019). Crop root system traits cannot be seen as a silver bullet delivering drought resistance. *Plant and Soil, 439*, 31-43.

Passioura, J. B. (1972). The effect of root geometry on the yield of wheat growing on stored water. *Australian Journal of Agricultural Research, 23*, 745-752.

Passioura, J. B. (1983). Roots and drought resistance. *Agricultural Water Management, 7*, 265-280.

Peleg, Z., Fahima, T., Abbo, S., Krugman, T., Nevo, E., Yakir, D., & Saranga, Y. (2005). Genetic diversity for drought resistance in wild emmer wheat and its ecogeographical associations. *Plant, Cell & Environment, 28*, 176-191.

Peleg, Z., Fahima, T., Krugman, T., Abbo, S., Yakir, D., Korol, A. B., & Saranga, Y. (2009). Genomic dissection of drought resistance in durum wheat x wild emmer wheat recombinant inbreed line population. *Plant, Cell & Environment, 32*, 758-779.

Percival, J. (1921). *The wheat plant. A monograph*

Pound, M. P., French, A. P., Atkinson, J., Wells, D. M., Bennett, M. J., & Pridmore, T. P. (2013). RootNav: navigating images of complex root architectures. *Plant Physiology, 162*, 1802-1814.

Preece, C., & Peñuelas, J. (2020). A return to the wild: Root exudates and food security. *Trends in Plant Science, 25*, 14-21.

R_Core_Team. (2020). R: A language and environment for statistical computing. R Retrieved from https://www.R-project.org

Rellan-Alvarez, R., Lobet, G., & Dinneny, J. R. (2016). Environmental control of root system biology. *Annual Reviews of Plant Biology, 67*, 619-642.

Richard, C., Hickey, L., Fletcher, S., Jennings, R., Chenu, K., & Christopher, J. (2015). High-throughput phenotyping of seminal root traits in wheat. *Plant Methods, 11*, 13.

Richards, R., & Passioura, J. (1989). A breeding program to reduce the diameter of the major xylem vessel in the seminal roots of wheat and its effect on grain yield in rain-fed environments. *Australian Journal of Agricultural Research, 40*, 943-950.

Robbins, N. E., II, & Dinneny, J. R. (2015). The divining root: moisture-driven responses of roots at the micro- and macro-scale. *Journal of Experimental Botany, 66*, 2145-2154.

Salazar-Henao, J. E., Vélez-Bermúdez, I. C., & Schmidt, W. (2016). The regulation and plasticity of root hair patterning and morphogenesis. *Development, 143*, 1848-1858.

Salvi, S., & Tuberosa, R. (2015). The crop QTLome comes of age. *Current Opinion in Biotechnology, 32*, 179-185.

Schneider, H. M., & Lynch, J. P. (2020). Should root plasticity be a crop breeding target? *Frontiers in Plant Science, 11,* 546.

Shorinola, O., Kaye, R., Golan, G., Peleg, Z., Kepinski, S., & Uauy, C. (2019). Genetic screening for mutants with altered seminal root numbers in hexaploid wheat using a high-throughput root phenotyping platform. *G3: Genes|Genomes|Genetics, 9,* 2799-2809.

Soriano, J. M., & Alvaro, F. (2019). Discovering consensus genomic regions in wheat for root-related traits by QTL meta-analysis. *Scientific Reports, 9,* 10537.

Strock, C. F., Burridge, J. D., Niemiec, M. D., Brown, K. M., & Lynch, J. P. (2020). Root metaxylem and architecture phenotypes integrate to regulate water use under drought stress. *Plant, Cell & Environment, in press*. doi:10.1111/pce.13875

Trachsel, S., Kaeppler, S. M., Brown, K. M., & Lynch, J. P. (2011). Shovelomics: high throughput phenotyping of maize (*Zea mays* L.) root architecture in the field. *Plant and Soil, 341,* 75-87.

Tracy, S. R., Nagel, K. A., Postma, J. A., Fassbender, H., Wasson, A., & Watt, M. (2020). Crop Improvement from phenotyping roots: Highlights reveal expanding opportunities. *Trends in Plant Science, 25,* 105-118.

Tyree, M. T., & Ewers, F. W. (1991). The hydraulic architecture of trees and other woody plants. *New Phytologist, 119,* 345-360.

Uga, Y., Sugimoto, K., Ogawa, S., Rane, J., Ishitani, M., Hara, N., . . . Yano, M. (2013). Control of root system architecture by *DEEPER ROOTING 1* increases rice yield under drought conditions. *Nature Genetics, 45,* 1097-1102.

Vadez, V., Kholova, J., Medina, S., Kakkera, A., & Anderberg, H. (2014). Transpiration efficiency: New insights into an old story. *Journal of Experimental Botany, 65,* 6141-6153.

Voss-Fels, K. P., Snowdon, R. J., & Hickey, L. T. (2018). Designer roots for future crops. *Trends in Plant Science, 23,* 957-960.

Watt, M., Fiorani, F., B., U., Rascher, U., Muller, O., & Schurr, U. (2020). Phenotyping: New windows into the plant for breeders. *Annual Review of Plant Biology, 71,* 689-712.

Watt, M., Magee, L. J., & McCully, M. E. (2008). Types, structure and potential for axial water flow in the deepest roots of field-grown cereals. *New Phytologist, 178,* 135-146.

Watt, M., Moosavi, S., Cunningham, S. C., Kirkegaard, J. A., Rebetzke, G. J., & Richards, R. A. (2013). A rapid, controlled-environment seedling root screen for wheat correlates well with

rooting depths at vegetative, but not reproductive, stages at two field sites. *Annals of Botany, 112*, 447-455.

Weaver, J. (1926). *Root development of field crops*. New York: McGraw-Hill.

Zadoks, J. C., Chang, T. T., & Konzak, C. F. (1974). A decimal code for the growth stages of cereals. *Weed Research, 14*, 415-421.

Zelko, I., Lux, A., Sterckeman, T., Martinka, M., Kollárová, K., & Lišková, D. (2012). An easy method for cutting and fluorescent staining of thin roots. *Annals of Botany, 110*, 475-478.